ORIGINAL ARTICLE

Development and Evaluation of Hesperidin-loaded Ethosomal Gel for Wound Healing

Hemant Bhati, Keshav Bansal, Meenakshi Bajpai

Department of Pharmaceutics, Institute of Pharmaceutical Research, GLA University, Mathura, Uttar Pradesh, India

Abstract

Background: Wound healing is a process that restores and regenerates the injured tissues. Polyphenols (Hesperidin) show wound healing properties, but their effective topical application for skin wound healing is challenging due to issues with low loading capacity and delivery efficiency. Ethosomes (lipid-based vesicles) have overcome such problems and emerged as a promising delivery system for improving drug encapsulation and penetration through the skin. **Materials and Methods:** Hesperidin-loaded ethosomes were formulated with 30% ethanol and analyzed for particle size and shape, encapsulation efficiency, and surface charge. Ethosomes gel was then formulated with 1% w/v Carbopol 934K. Further Hesperidin-loaded ethosomal gel was evaluated for various parameters such as organoleptic properties, pH, viscosity, and skin permeation. An *in-vitro* wound healing assay was performed to assess the angiogenic properties of Hesperidin-loaded ethosomal gel along with its comparison with pure Hesperidin. **Results:** The formulated ethosomes were found to have a spherical shape, a vesicle size of 417.9 nm, an entrapment efficiency of 87.32%, and a surface charge of −26.62 mV. The ethosomal gel showed an optimal pH of 5.7, good spreadability, and a release of 86.21%. It has shown stability over 60 days. *In-vitro* assay revealed that both Hesperidin-loaded ethosomal gel and powder exhibited angiogenic effects, significantly promoting angiogenesis in HaCaT cells over time. **Conclusion:** The development of Hesperidin-loaded ethosomal gel has successive delivery and addressed the challenges of high loading capacity and effective skin permeation. The results suggest that Hesperidin-loaded ethosomal gel is an effective method for enhancing wound healing through improved delivery.

Key words: Ethosome gel, HaCaT cell, hesperidin, polyphenol, skin permeation, wound healing

INTRODUCTION

It is well acknowledged that skin injuries are among the most common type of physical harm. People who are receiving radiation treatment or have diabetes often get persistent wounds that heal slowly.[1] The formation of clots, inflammation, proliferation, and remodeling are all part of the wound healing process. The body releases the growth factor to accelerate the healing process, which stimulates platelets to form a clot and initiates hemostasis to stop bleeding.[2,3] To remove injured tissue, neutrophils produce protease, and antimicrobial compounds as part of an inflammatory response that follows. Macrophages, which are essential for phagocytizing germs, dead neutrophils, and injured tissues, develop from monocytes around 3 days after injury.[4,5] Furthermore, macrophages aid in angiogenesis and the formation of vascularized connective tissue, leading to wound closure.[6] The remodeling phase begins during proliferation and continues for a long period. Due to their physical properties, such as swelling and biodegradability, hydrogels possess many ideal qualities for wound dressings.

Drug therapy has been employed to enhance scaffold efficacy in promoting neural function recovery.[7] Hesperidin, a natural bioflavonoid found abundantly in citrus fruits such as sweet oranges and lemons, has been noted for its broad pharmacological properties, including anti-inflammatory, antioxidant, antimicrobial, and anticancer effects, as well

Address for correspondence:
Dr. Keshav Bansal, Institute of Pharmaceutical Research, GLA University, Mathura, Uttar Pradesh, India.
Phone: +91 9997592453.
E-mail: keshav.bansal@gla.ac.in

Received: 04-02-2025
Revised: 15-05-2025
Accepted: 25-05-2025

as its potential in treating neurodegenerative diseases.[5,8] Herbal medications often face issues with their therapeutic potential due to the larger size of bioactive particles, which hampers their ability to cross lipid membranes and raises solubility concerns.[9,10] These factors negatively impact drug bioavailability. Transforming conventional doses of Hesperidin into nanoformulations through nanotechnology provides several benefits, such as enhanced solubility, bioavailability, permeability, stability, and therapeutic outcomes.

Transdermal or intradermal drug administration can bypass systemic constraints like first-pass metabolism in the lungs, liver, or gastrointestinal tract, ensuring the drug reaches its target more effectively.[11,12] This method offers several advantages by delivering the drug through the skin at a controlled rate via passive diffusion, optimizing systemic effects. To achieve this, drugs are encapsulated in "skin-friendly" nano vectors, often using lipid-based vesicular systems.[13,14] Ethosomes, the latest innovative, non-invasive, passive carriers for lipid-based systems, exhibit promising characteristics. These soft, flexible phospholipid vesicles are designed for improved drug delivery, consisting of multiple concentric layers of phospholipid, water, and a high concentration of ethanol.[15] Ethosomes enhance drug penetration through the stratum corneum barrier, reaching deeper skin layers compared to liposomal methods. The ethanol's effect on the stratum corneum, combined with the vesicle's deformability and permeability, facilitates this enhanced penetration. The fluidity of ethanol and lipid molecules in the polar head region further increases membrane permeability. Therefore, ethosomes are regarded as superior carriers for transdermal drug delivery systems due to their unique characteristics.[16,17]

Quality by design is a robust method for optimizing pharmaceutical nanoformulations using analysis of variance (ANOVA) or one-way assessment of variance statistics to design studies and interpret variable effects.[18,19] The objective of this study was to improve the drug release by incorporating Hesperidin into ethosomal gel, comparing the outcomes to various experimental doses, and to determine the best optimum formula for testing the wound healing activity.

MATERIALS AND METHODS

Hesperidin was bought from Yarrow Chem, Mumbai, India. Central Drug House (P) Ltd., Delhi, India, supplied soya lecithin, cholesterol, propylene glycol (PG), iso-propylene alcohol, and carbopol-934 was provided by Chemdyes Corporation, Gujarat, India. Analytical-grade chemicals and double-distilled water were used throughout the experiments. The HaCaT (Huma Skin Keratinocytes) were purchased from NCCS, Pune, India. The cells were kept in a CO_2 incubator at 37°C with 5% CO_2, 18–20% O_2, high glucose medium supplemented with 10% fasting blood sugar, 2 mM glutamine, and 1% antibiotic-antimycotic solution. The cells were subcultured every 2 days. For this study, HaCaT cells with a passage number of 72 were used.

Preformulation and physicochemical characterization

Characterization of hesperidin

It is essential to be aware of the drug's various physiochemical characteristics (preformulation study) before developing any dosage form, which helps the formulator in developing an attractive, reliable, potent, and secure dosage form.[20,21]

Melting point (MP) determination

A digital MP instrument (model number BTL.40, Navyug, India) was used with the capillary for the determination of the MP of Hesperidin.[22]

Fourier transform infrared spectroscopy (FT-IR) analysis

FTIR analysis was performed to identify the active functional groups in the drug by using an attenuated total reflectance (ATR)-FTIR spectrophotometer (Shimadzu IR-Sprit-T).[23,24]

Formulation of ethosomes incorporated with hesperidin

The ethosomes loaded with Hesperidin were formulated by using the approach outlined by Touitou *et al*.[25] As shown in Table 1, all required ingredients were weighed in different

Table 1: Composition and response in CCD for ethosomal gel by two independent variable optimizations using design expert software

Run	Independent variable		Dependent variable	
	Amt. of soya lecithin (mg)	Amt. of ethanol (mL)	Particle size (nm)	Entrapment efficiency (%)
1	400.00 (high)	25.00	463.25	65.32
2	137.00	25.00	295.35	63.85
3	100.00 (low)	10.00 (low)	280.77	55.82
4	250.00	25.00	358.85	75.25
5	250.00	25.00	375.36	76.65
6	400.00	10.00	485.5	63.35
7	250.00	25.00	365.5	79.35
8	300.00	30.00	417.9	87.32
9	250.00	40.00	401.32	80.24
10	400.00	40.00 (high)	465.35	70.25
11	250.00	25.00	375.25	78.35
12	100.00	40.00	250.89	59.32
13	250.00	10.00	381.2	79.35

CCD: Central composite design

concentrations to prepare the ethosomal formulation. Initially, Hesperidin and soy lecithin were mixed with ethanol and PG. The mixture was kept in a water bath at 30°C, and then distilled water was added to the mixture while continuously stirring at 700 revolutions per minute in a sealed jar using a magnetic stirrer (Remi Equipment, Mumbai). The resulting solution was maintained at 4°C. Next, sonication was performed 3 times using a probe sonicator, each lasting approximately 5 min with a 5-min interval between each session.[26] Each formulation was visually inspected for homogeneity, ensuring no precipitation or phase separation occurred. The most suitable formulation was then subjected to detailed analysis.[27]

Experimental design

Design expert software (DES) was used statistically to analyze the experimental design. The response surface design that was most often employed was central composite design (CCD). As shown in Table 1, the amount of soya lecithin and ethanol were chosen as independent variables with two levels. Using the 2–2 design for ethosome optimization, the effects of independent components, such as lecithin (X1), and ethanol (X2), on dependent variables, such as particle size (PS), and entrapment efficiency (EE), were examined. The goal was to maximize EE by optimizing the independent factors. To evaluate the significant model, an ANOVA model was used.

Characterization of ethosomes

Vesicle size, zeta potential (ZP), and polydispersity index (PDI) analysis

The Malvern Zetasizer (Nano ZS, Malvern, UK) was used in the dynamic light scattering (DLS) technique to estimate the vesicle's size, ZP, and PDI.[28,29]

FTIR analysis and morphological study of ethosomes-loaded hesperidin

The ethosomes were analyzed using ATR-FTIR, as mentioned above. Transmission electron spectroscopy (TEM) (Talos L120C TEM) was used to evaluate the morphology of the formulation by utilizing a ×9,000 and 200 kV magnifiers.[30]

EE determination

EE is the total amount of drug contained in formulation vesicles. To separate the unentrapped drug, a cooling centrifuge running at 16,000 rpm at 4°C was used.[31] The supernatants were diluted with distilled water (10 mL, 3 min).[32]

$$EE = \frac{\text{Amt. of incorporated drug} - \text{Amt. of free drug present}}{\text{Amount of incorporated drug}} \times 100$$

Statistical analysis

The outcomes were expressed as mean ± standard deviation, and measurements were made in triplicate. For every response factor, including interactions and quadratics, multiple linear regression analysis generates polynomial models. Interaction coefficients were calculated and equations were generated to examine how each variable affected the formulation's characteristics. A variance analysis was carried out in order to verify the model. With DES, three-dimensional response graphs were produced.[33]

Characterization of ethosomal gel

Estimation of pH, viscosity, spreadability, and extrudability

A digital pH meter was used to determine composition.[34] By submerging a Brookfield viscometer (LVDV-II pro) spindle of S-96 at different rpm (10, 15, and 20) for various periods at the lower, medium, and higher case into a beaker containing ethosomal gel, the viscosity of the formulation was determined.[35]

To test the spreadability of the gel, 1 g of ethosomal gel was weighed and placed between two 8 cm long glass slides. The weight at which the glass slide shifted out of place was identified by attaching different weights to the pulley. The time required for the gel to reach the bottom slide and to move the top slide was also noted. After completing three measurements, the readings were calculated using the following formula:

$$S = M\frac{L}{T}$$

Where, S = Spreadability of ethosomal gel; M = Weight (g) tide to upper slide; L = Distance (cm) moved by slide; and T = Time taken by upper slide to move downwards.

After 20 g of prepared ethosomal gel was placed into tubes (collapsible tubes), pressure was applied, extrudability resulted. To stop the medicament from flowing backward, a clamp was attached to the tube. After opening the tube, the quantity of gel was calculated and recorded that kept extruding until the pressure persisted.

In-vitro drug release

To perform the *in vitro* permeation assessment investigation, an egg membrane equipped with a modified Franz diffusion cell was used. For this investigation, a pH 6.8 phosphate buffer saline was used. The formulation, which is comparable to 2.5 mg of medication, was applied onto the skin (upper side of the skin). A consistent 37 ± 2°C temperature was maintained during the assembly. Using sampling tubes, the samples were taken from receptor media once an hour, and

add equivalent amount of fresh receptor media was used at the same time to generate skin condition. Using an appropriate blank, the solutions were measured at 286 nm using a UV spectrophotometer (Shimadzu-1,800). Each formulation went through a similar procedure, and at the conclusion, a graph was made showing the relationship between time and the total drug release percentage. Each ethosomal formulation had three runs of the experiment, and the findings were given as mean ± SD.[35,36]

In-vitro wound healing assay

Wound healing assay was performed on normal human keratinocyte (HaCaT) cells. A broad range of experimental settings, such as gene knockdown or chemical exposure, have been studied in relation to the migration and proliferation of mammalian cells using the scratch wound healing assay. To perform a wound healing assay, place the cell at a density of 0.25 million per well in a 12-well tissue culture plate, and let them a day to grow to 80–100% confluence. Scratch the monolayer using a new 200 µL pipette tip without changing the medium, and ensure the tip is perpendicular to the well bottom to create a consistent gap. In each well, scratch another line perpendicular to the first to develop a cross and wash it twice with medium to remove detached cells. Treat the cells with desired concentrations of test compounds and incubate at 37°C with 5% CO_2. Include untreated cells as a control. Continue incubation for 72 h or the required duration for different cell types. Capture images at adequate intervals (e.g., 0, 24, 48, and 72 h) using consistent microscope settings. Quantify the gap distance using software like Image J, ensuring multiple views of each well are documented, and experiments are repeated to reduce variability.[37,38]

$$\%\,\text{of Wound Healing Scored} = \frac{(\text{Initial area} - \text{Final area})}{\text{Initial area}} \times 100$$

RESULTS

Preformulation studies

MP

The MP of Hesperidin was recorded to be 260.3°C; at this temperature, the drug has started to decompose.

FTIR analysis

Table 2 provides the spectrum interpretation for each sample. The main peaks in the hesperidin-loaded ethosomal system were nearly identical to those in the pure drug, suggesting that there was no significant interaction between the drug and the other excipients in the distributed system. Figure 1 displays the FTIR spectra of the pure drug. The peak observed at 3723.34 and 3412.10 cm^{-1} corresponds to O–H stretching vibration. The peak at 2516.42 and 3942.49 cm^{-1} demonstrates the presence of C-H stretching, the peak at 1631.12 cm^{-1} shows C=O stretching, and 1399.42 cm^{-1} shows C-O stretching in the sample.

Table 2: Spectral interpretation of hesperidin through FTIR spectroscopy

S. No.	Frequency (cm^{-1})	Frequency of reference (cm^{-1})	Assignment
1	3723.34 3412.10	3,800–3,000	O-H (stretching)
2	2516.42 2924.49	3,300–2,500	C-H (stretching)
3.	1631.12	1,700–1,630	C=O (stretching)
4.	1399.42	1,400–1,000	C-O (stretching)

FTIR: Fourier transform infrared spectroscopy

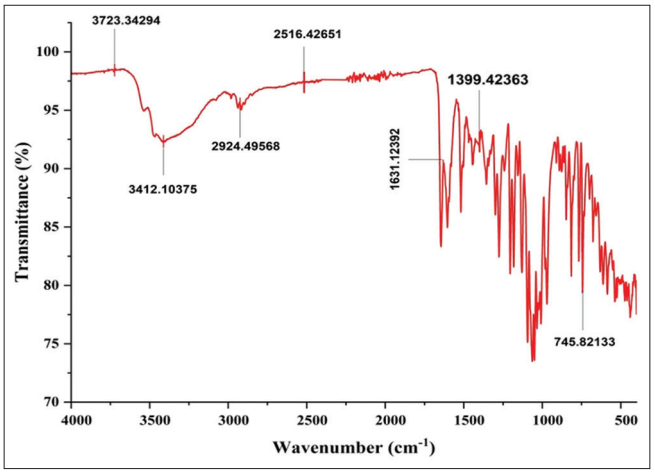

Figure 1: Fourier transform infrared spectroscopy spectrum of hesperidin

Visualization of ethosomal vesicles

Determination of PS, ZP, and PDI

Based on DLS, the PS was estimated. Table 3 presents the results for both PS and PDI. The PS of the prepared ethosomal formulation was found to be 280.77–485.5 nm, and PDI was in the range of 0.324–0.613, with an optimal PS and PDI of 417.9 nm and 0.459, respectively [Figure 2]. On the other hand, formulation F10 shows the highest values for PDI and PS, which are 465.35 and 0.613, respectively. The vesicle's size is particularly important when it comes to the topical delivery of drugs. The study revealed that there is an abrupt increase in the formulation's PS when the concentrations of soya lecithin are raised over 300 mg. Thus, it can be inferred from the previous statement that changing the ratio of lipid to ethanol affects the formulation's physical characteristics in one way or another. Furthermore, the rate at which the formulation penetrates the skin can be influenced by the size of the particles and the quantity of ethanol. The smaller

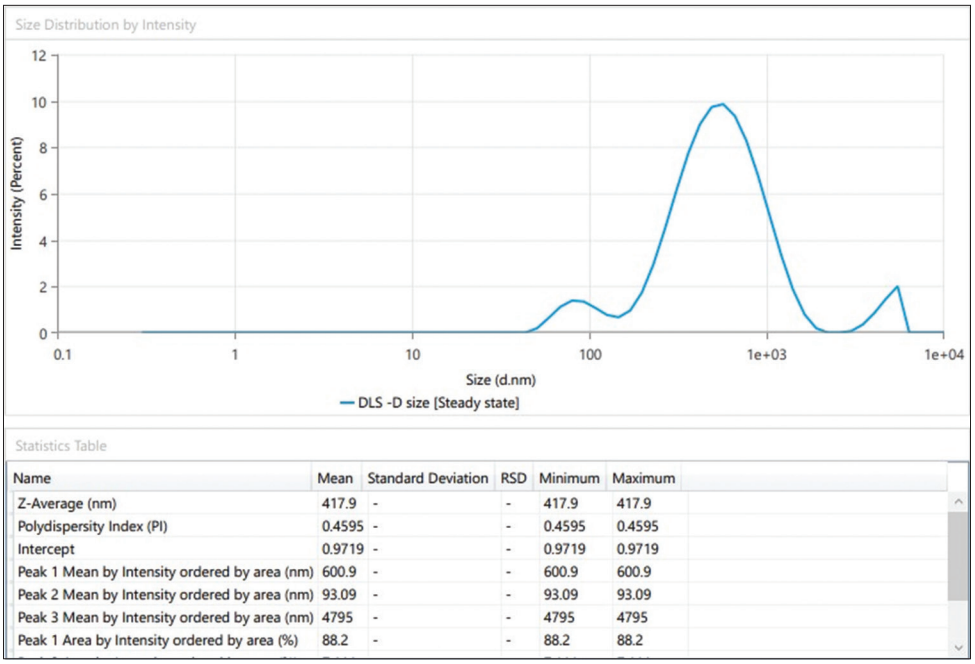

Figure 2: Size of optimized formulation

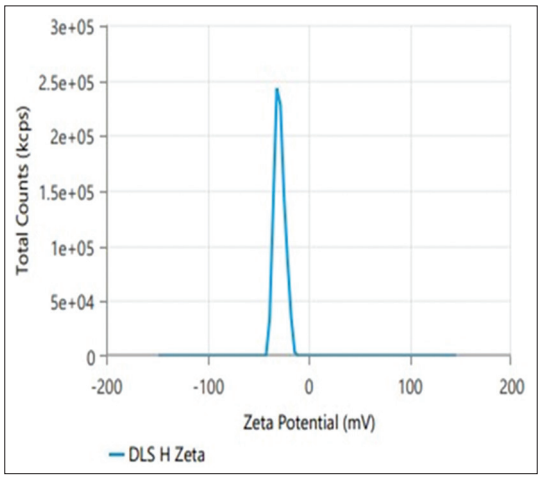

Figure 3: Zeta potential of optimized formulation

the size of the vesicle, the more effectively it penetrates the content into underlying layers of the skin. Based on the above-mentioned results, formulation F8 demonstrated an optimal PS of about 417.9 nm, indicating great suitability for topical administration.

The stability of the ethosomal formulation is assessed using the ZP. Table 3 lists the ZP values, which ranged from −11.6 to −35.6 mV. ZP has a maximum value represented by F6, which is −35.6 mV, and a minimum value represented by F4, which is about −13.6 mV [Figure 3]. Formulations F1, F2, and F3 showed no significant change in the ZP values, that is −18.6, −17.9, and −18.5.

Experimental design and optimization of ethosomal formulation

Phospholipid and ethanol were chosen as independent variables, while PS and EE were examined as dependent variables. CCD was utilized to study these factors at two levels. Table 1 shows the formulations prepared in 13 batches, along with the summaries of their responses.

Table 3: EE, PS, PDI, and ZP of prepared ethosomal formulation

Code	EE (%)	PS (nm)	PDI	ZP
F1	65.32	463.25	0.482	−18.6
F2	63.85	295.35	0.324	−17.9
F3	55.82	280.77	0.525	−18.5
F4	75.25	358.85	0.542	−13.6
F5	76.65	375.36	0.447	−13.9
F6	63.35	485.5	0.336	−35.6
F7	79.35	365.5	0.403	−20.19
F8	87.32	417.9	0.4595	−28.62
F9	80.24	401.32	0.459	−18.9
F10	70.25	465.35	0.342	−13.7
F11	78.35	375.25	0.497	−15.4
F12	59.32	250.89	0.613	−14.6
F13	79.35	381.2	0.432	−15.8

EE: Entrapment efficiency, PS: Particle size, PDI: Polydispersity index, ZP: Zeta potential

Effect of variables on PS

In order to determine a connection between the various analyzed responses and the investigated variables, data were processed to fit complete second-order cubic or quadratic polynomial equations with extra interaction components. The plots in [Figure 4a] depicted that an optimum level of lecithin and an increased level of ethanol have a favorable impact on the size of particles. PS was shown to rise with

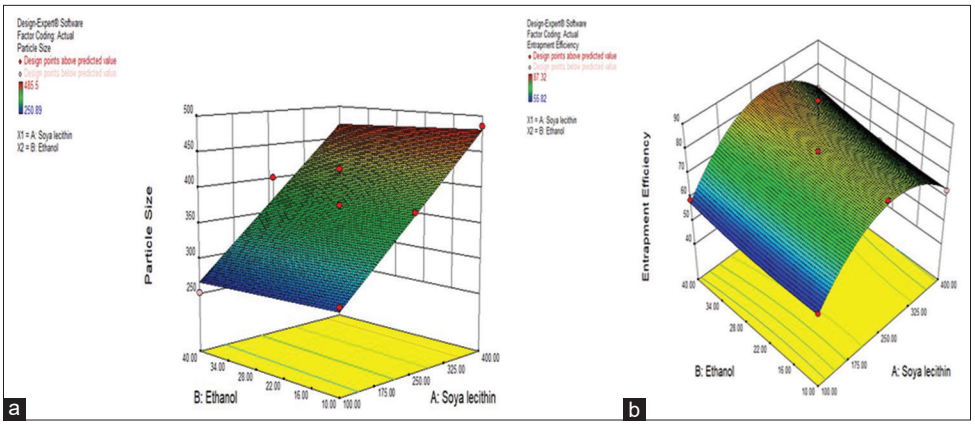

Figure 4: 3-dimensional response surface graph indicating the impact of independent variables (phospholipid and ethanol) on these (a) particle size (nm) and (b) entrapment efficiency (%)

soya lecithin content while maintaining a fixed ethanol concentration.

The quadratic equation generated by the software is:

PS = + 376.56 + 96.10 * A + 1.34 * B

The model terms were significant, as shown by the ANOVA results with $P < 0.0001$. The model is likely significant based on its F-value of 167.05. The adjusted determination coefficient (R2) was 0.9651, and the predicted determination coefficient (R2) was 0.9492. At a signalto-–noise ratio of 21.877, the signal is sufficient.

Effect of variables on EE

The 3D figure demonstrated a clear correlation between the drug's EE and phospholipid and ethanol concentration [Figure 4b]. Equation (2) shows the final mathematical model for EE, based on coded parameters calculated by DES.

EE = + 78.80 + 5.25 * A + 2.31 * B + 1.06* A * B −18.13* A^2 +1.49 *B^2

Table 4 demonstrates that the EE of linear and quadratic models has significant *P*-values. The ANOVA results demonstrated $P < 0.0010$, indicating that the model terms are significant. The F-value of 16.03 implies the model is significant. The signal-to-noise ratio of 11.048 indicates an adequate signal.

Desirability function

The current study showed PS ranging from 280.55 to 480.77 nm. The ethosomal formulation with a desirability value of 1 was chosen as the optimized formulation, which contained 300 mg of phospholipid and 30 mL of ethanol. Table 5 compares the experimental values of PS and EE of the optimized ethosomal formulations with the predicted value and calculates the percentage bias.

$$\text{Percent bias} = \frac{(\text{Predicted value} - \text{Experimental value})}{\text{Predicted value}} \times 100$$

Table 4: Summary of the model fit for the response (PS and EE)

S. No.	Source	PS		EE	
		F-value	*P*-value	F-value	*P*-value
1	Mean versus linear	167.05	<0.0001	0.71	0.5136
2	Linear versus 22FI	0.93	03590	0.057	0.8174
3	Quadratic versus 2F1	3.75	0.0780	34.39	0.0002
4	Cubic versus quadratic	1.89	0.3148	5.92	0.0879

EE: Entrapment efficiency, PS: Particle size

Table 5: Percentage biasness

Responses	Predicted values	Experimental values	Bias (%)[a]
Particle size (nm)	376.56	417.9	−2.06
Entrapment efficiency (%)	78.79	87.32	−4.53

Percentage bias = *(Predicted value-Experimental value)/ Predicted value x 100

EE

The EE of the hesperidin-loaded ethosomal system directly affects the delivery potential. Table 1 displays the results of the determination of each formulation's EE. The formulation developed with 300 mg soyalecithin and 30 mL ethanol demonstrated maximum EE, i.e., 87.32%. This could be because of the increased ethanol content, which makes the drug more soluble in ethosomes.

Characterization of optimized ethosomal formulation

Morphology

TEM [Figure 5] images reveal information on the spherical shape of the particles in the formulation in addition to surface

morphology. Images acquired using TEM demonstrated that the ethosomes had a spherical form, were smooth, free from crystallinity, and were within the nanometer range. The average PS, calculated using Image J software, was 59.91 ± 43.75 nm. However, the mean PS measured by DLS was significantly larger at 417.9 nm. This discrepancy may be because DLS measures the hydrodynamic diameter, which includes both the core of the particle and the solvent layer attached to the particles. TEM sample preparation comprises drying, dehydration, staining, and electron irradiation of ethosomes, resulting in shrinkage of the particles, as described in previous publications.[39] Previous investigations reported similar variances in PS.[40]

Ethosomal gel characterization

The optimized ethosomal gel containing Hesperidin-loaded ethosome was assessed for organoleptic properties (odor, color, and phase separation), pH, and viscosity.

Evaluation of organoleptic properties

The homogeneity and organoleptic properties did not change at various temperatures over the stability investigations allotted duration. At a higher temperature, the light brown color of all the formulations changed to a dark brown color.

FTIR spectroscopy

The FTIR spectra of Hesperidin, soya lecithin, ethanol, cholesterol, physical mixture, ethosomes, and gel are shown in Figure 6. The FTIR spectra of Hesperidin [Figure 1] showed O-H stretching at 3723.34 and 3412.10 cm^{-1}, the peak at 2516.42 and 3942.49 cm^{-1} demonstrates the presence of C-H stretching, the peak at 1631.12 cm^{-1} shows C=O stretching and 1399.42 cm^{-1} shows C-O stretching in the sample were observed in agreement with the previously reported values. The soya lecithin spectrum showed peaks at 3,409 cm^{-1} (OH stretching), 1,698 cm^{-1} (C=O stretching), and 1,062 cm^{-1} (C-O stretching). Ethanol showed peaks at 3,391 cm^{-1} (OH stretching), 2,961 cm^{-1} (CH stretching), and 1,055 cm^{-1} (CO stretching). Carbopol displayed peaks at 3,422 cm^{-1} (OH stretching), 2,932 cm^{-1} (CH stretching), and 1,724 cm^{-1} (C=O stretching). Cholesterol exhibited peaks at 2,936 cm^{-1} (CH stretching), 1,464 cm^{-1} (CH bending), and 1,056 cm^{-1} (CO stretching). The spectrum of the PM included all the characteristic peaks of Hesperidin, lipid, ethanol, and carbopol, indicating no interaction. The gel containing the optimized ethosomal formulation showed good solubilization of the drug in lipid and ethanol, as indicated by the reduced intensity and broadening of the peaks, thus demonstrating the EE of the drug in the formulation.

Viscosity, pH, spreadability, and extrudability

The viscosity and pH of all ethosomal formulations ranged from 5,435 to 8,954 cps and 6.5 to 5.7, and Table 6 shows the results for all formulations, including excellent values for spreadability and extrudability. The results indicate that the

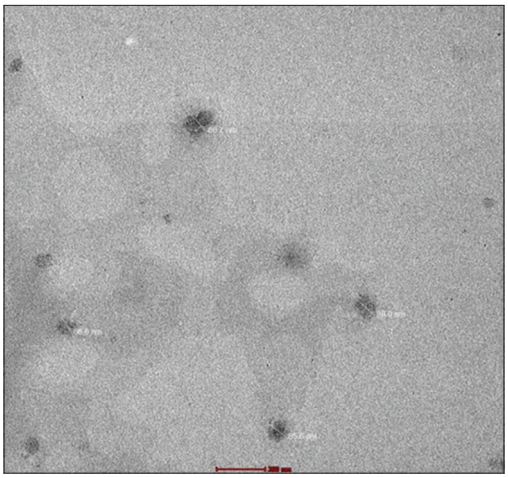

Figure 5: Transmission electron spectroscopy of optimized formulation

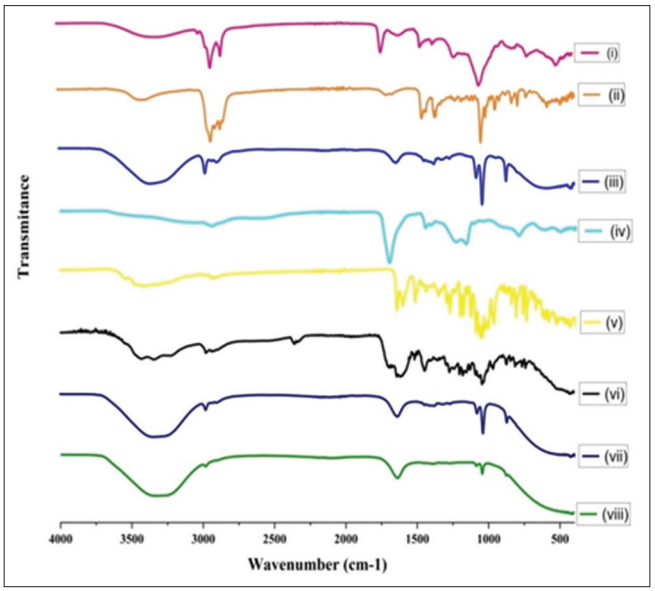

Figure 6: Fourier transform infrared spectroscopy spectra of (i) Soya lecithin, (ii) Cholesterol, (iii) Ethanol, (iv) Carbopol, (v) Hes, (vi) Physical mixture, (vii) Ethosomes (viii) Ethosomal gel

formulation is appropriate for topical use. The formulation F3 had optimal pH, viscosity, and spreadability, indicating superior gelling properties for topical application.

In-vitro release studies

The *in vitro* release profiles of the ethosomal gel with different concentrations of Carbopol are shown in Figure 7. The ethosomal gel with a concentration of 1% Carbopol showed a maximum release of 86.21% after 24 h.

In-vitro wound healing assay

The wound healing effect of Hesperidin-loaded ethosomal gel and Hesperidin powder was studied till 72 h of incubation, about more than 90% of the scratched area were closed since the

Table 6: pH, viscosity, Spreadability, and extrudability of prepared ethosomal gel containing different concentrations of Carbopol

Formulation	pH	Viscosity	Spreadability	Extrudability
F1	6.4	5435	7.12±0.3	+++
F2	5.7	5867	6.84±0.2	++
F3	6.2	7128	6.83±0.4	+++
F4	6.5	8120	5.56±0.6	++
F5	5.8	8954	4.33±0.8	+

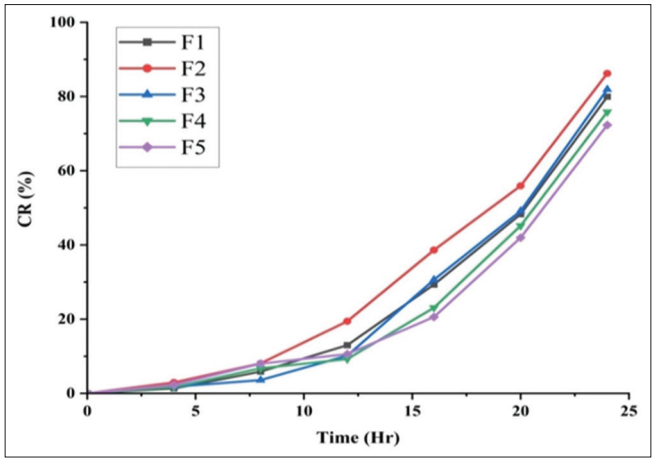

Figure 7: *In-vitro* release profile of ethosomal gel with different concentrations of Carbopol

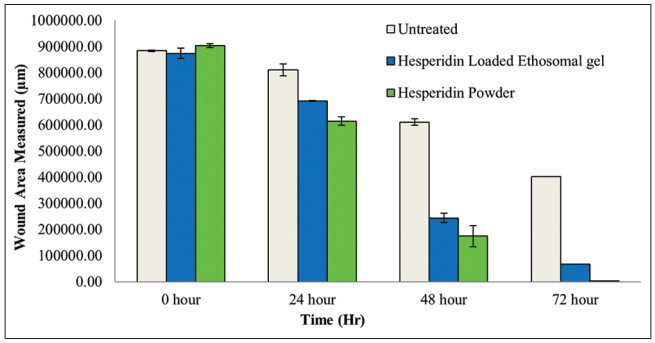

Figure 8: Covered wound area overlay-hesperidin loaded ethosomal gel and hesperidin powder

HaCaT cells had proliferated and migrated into the scratched area [Figure 8], and the treatment group cells achieved about >90% wound healing rate that has been shown in Figure 9. The description of wound area covered and % wound closure scored in terms of area is described in Tables 7 and 8, respectively. Overall the observed wound healing study results confirmed that given test compounds, Hesperidin-loaded ethosomal gel and Hesperidin powder with 50 ug/mL effectively enhanced the wound healing effect on HaCaT cells after 72 h of incubation in time time-dependent fashion. The statistical data of the covered wound area is shown in Figure 10. In summary, its evidently proved that Hesperidin-loaded ethosomal gel and Hesperidin powder molecules were angiogenic in nature in a time-dependent fashion and it effectively promoted the angiogenic properties on HaCaT cells.

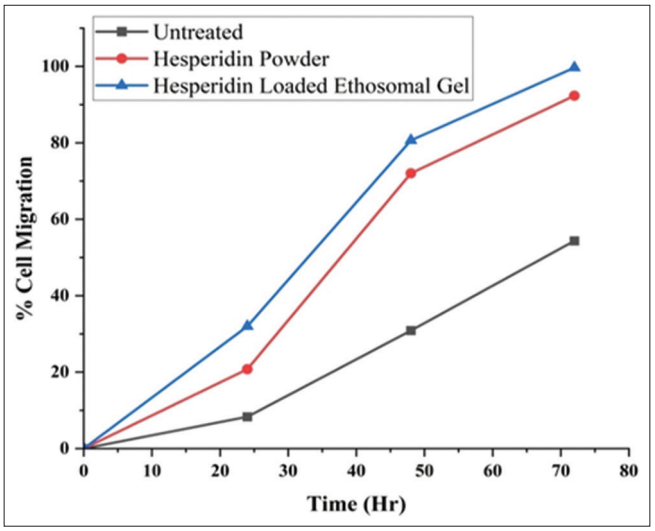

Figure 9: Percentage wound closure in HaCaT cells

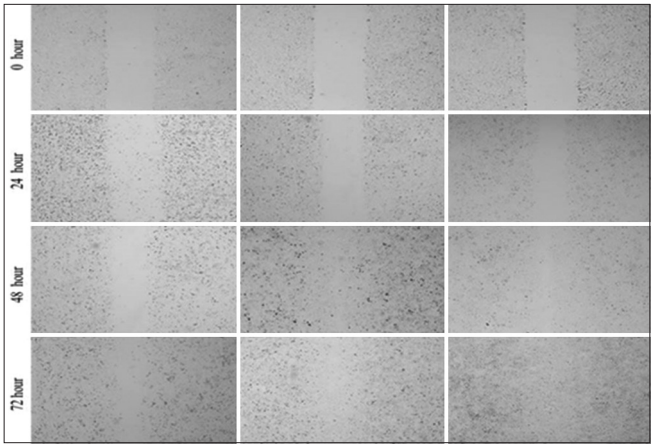

Figure 10: *In-vitro* wound healing activity of Hesperidin loaded ethosomal gel and hesperidin powder 50 µg/mL at different time intervals of 0 h, 24 h, 48 h, 72 h on HaCaT cells along with controls. (a) Untreated, (b) Hesperidin Powder-50 µg and (c) Hesperidin loaded ethosomal Gel-50 µg

Stability studies

Stability tests were used to assess the ethosomal system's ability to adhere to the drug. Table 9 shows the stability of selected ethosomal gel by using different parameters, including color, odor, and phase separation. Figure 11 depicts the pH of ethosomal gel at different temperatures.

Table 7: *In-vitro* wound healing effect of hesperidin powder and hesperidin loaded ethosomal gel against the HaCaT cells at different intervals in terms of area. The presented values were the average of 3 independent individual experiments (*n*=3)

Incubation Time	Wound area covered		
	Untreated	Hesperidin powder	Hesperidin loaded ethosomal gel
0 h	884056±6097	904379±12692	873895±34669
24 h	810553±38802	615043±27550	692432±3527
48 h	610969±21165	175145±71338	244388±31747
72 h	403516±5700	2907±999	67207±90415

Table 8: *In-vitro* wound healing effect of hesperidin loaded ethosomal gel and hesperidin powder with 50 ug/mL against the HaCaT cells at different intervals in terms of percentage. The presented values were the average of 3 independent individual experiments (*n* = 3)

Incubation time (h)	Percentage wound closure scored		
	Untreated	Hesperidin powder	Hesperidin loaded ethosomal gel
0	0.00	0.00	0.00
24	8.31	20.76	31.99
48	30.89	72.03	80.63
72	54.36	92.31	99.68

Table 9: Evaluation of organoleptic stability of ethosomal gel at different temperatures

Parameter	Temp	Initial	7 days	15 days	30 days	60 days	90 days
Color	4	Light brown	Light brown	Light brown	Light brown	Light brown	Light brown
	25	Light brown	Light brown	Light brown	Light brown	Light brown	Brown
	40	Light brown	Light brown	Brown	Brown	Brown	Dark brown
Odor	4	-	-	-	-	-	-
	25	-	-	-	-	-	-
	40	-	-	-	-	-	-
Phase separation	4	-	-	-	-	-	-
	25	-	-	-	-	-	-
	40	-	-	-	-	-	-

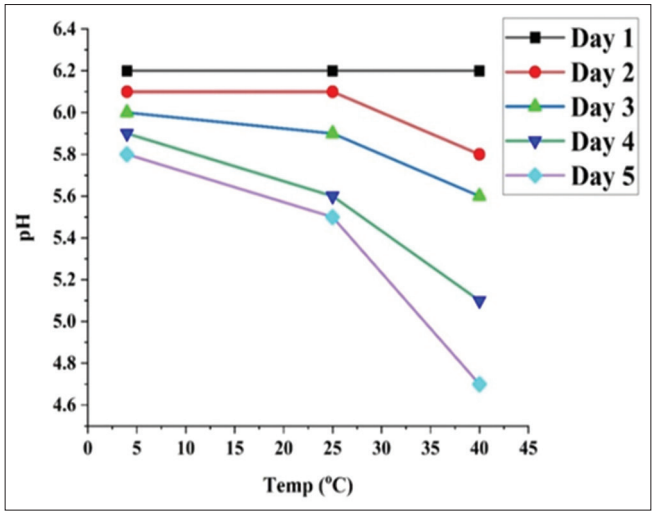

Figure 11: Effect of pH of ethosomal gel at different temperatures

As temperature rises, molecular vibrations and ionization accelerate, leading to a decrease in pH. It is possible that at higher temperatures, there is less polymer entanglement. However, the shift has not been drastic. Figure 12 depicts the viscosity of ethosomal gel at different temperatures. Stability studies show that viscosity reduces as temperature increases. The study concludes that carbopol-based ethosomal gel is thermally stable.

DISCUSSION

Herbal ethosomal gel was formulated by incorporating Hesperidin. To demonstrate the formulation's efficacy and suitability, it underwent a series of characterizations. The FTIR studies of the pure drug revealed the presence of important groups that are helping in wound healing.[41,42] Vesicles of around

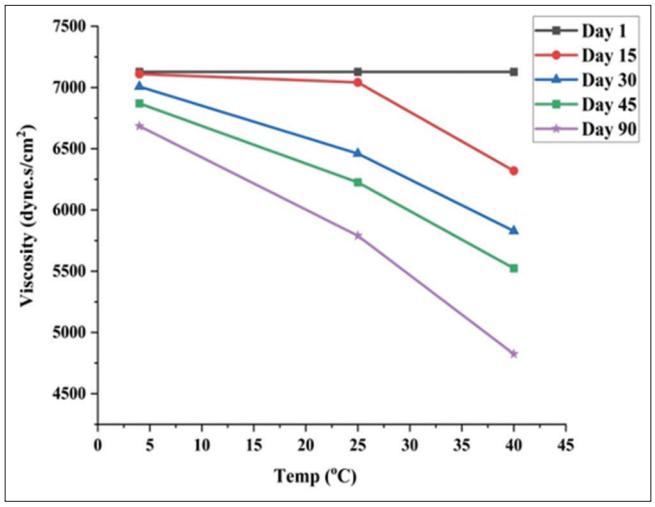

Figure 12: Effect of viscosity of ethosomal gel at different temperatures

420 nm can penetrate deeper layers of skin. In an analysis of the PS and PDI, it has been observed that the amount of soya lecithin is directly correlated with the vesicle size. An increase in soya lecithin concentration beyond 300 mg is associated with an abrupt increment in the PS and narrow distribution of PDI.[43] PG may allow penetration into deeper layers of the skin. Therefore, it can be inferred that alterations in the ratio of lipids to ethanol, either increased or decreased, significantly affect the physical characteristics of ethosomes. PS and the concentration of ethanol have an impact on the skin's permeability since only smaller particles can pass through it, while ethanol concentration typically has an impact on a drug's permeability.[44,45] With the foregoing considerations, we may conclude that F8 is entirely appropriate for skin administration. Further, in the case of ZP, research revealed that particles will encounter repulsion among themselves and resist agglomeration if the suspension contains a high amount of cationic and anionic charge in the system (i.e., a high value of both positive and negative ZP).[46] Consequently, increased surface charge improves the stability of ethosomes. The above-mentioned statement indicates that F8, with its greatest ZP value, has the best level of stability compared to the remaining formulations. PDI values above 0.7 suggest the existence of bigger particles in ethosomal dispersions and a heterogeneous system. The present system has a homogeneous and narrow PS distribution, as shown by the majority of the values. The stability studies confirmed that the prepared ethosomal gel was thermally stable.

CONCLUSION

Development of an appropriate carrier system for dermal delivery of Hesperidin was highly difficult due to its hydrophilic nature, leading to limited skin liberation. Due to the substantial amount of ethanol in their composition, ethosomes have been found to provide both continuous skin permeability and enhanced medication permeability through lipid vesicles. A stable gel containing ethosomes of nanometer range loaded with Hesperidin increased the penetration to the skin and could be a potential product for researchers.

The present study focuses on developing and evaluating a hesperidin loaded ethosomal gel to stimulate wound healing through enhanced skin penetration. Ethosomes, flexible lipid-vesicles, were formulated using 30% ethanol to encapsulate hesperidin, offering better drug delivery across the skin barriers. The formulated ethosomes demonstrate an average vesicle size (417.9 nm) along with better EE (87.32%) and surface charge (−26.62 mV). The ethosomal gel unveiled optimal attributes including pH (5.7), release rate (86.21%) and good spreadability. *In-vitro* wound healing assay demonstrated that hesperidin loaded ethosomal gel and powder significantly promoted angiogenesis in HaCaT cells. The obtained results favoured gel formulation, indicating their enhanced potential towards wound healing.

ACKNOWLEDGMENT

The authors would like to acknowledge the Institute of Pharmaceutical Research, GLA University, Mathura for providing the necessary facilities.

AUTHORS' CONTRIBUTIONS

All authors have accepted responsibility for the manuscript's content and consented to its submission. They have thoroughly reviewed all results and unanimously approved the final version of the manuscript.

REFERENCES

1. Yang X, Ren H, Guo X, Hu C, Fu J. Radiation-induced skin injury: Pathogenesis, treatment, and management. Aging (Albany NY) 2020;12:23379-93.
2. Meng X, Lu Y, Gao Y, Cheng S, Tian F, Xiao Y, *et al*. Chitosan/alginate/hyaluronic acid polyelectrolyte composite sponges crosslinked with genipin for wound dressing application. Int J Biol Macromol 2021;182:512-23.
3. Ghobashy MM, Elbarbary AM, Hegazy DE, Maziad NA. Radiation synthesis of pH-sensitive 2-(dimethylamino) ethyl methacrylate/polyethylene oxide/ZnS nanocomposite hydrogel membrane for wound dressing application. J Drug Deliv Sci Technol. 2022;73:103399.
4. Poonguzhali R, Basha SK, Kumari VS. Synthesis and characterization of chitosan-PVP-nanocellulose composites for *in-vitro* wound dressing application. Int J Biol Macromol 2017;105:111-20.
5. Fernández-Guarino M, Hernández-Bule ML, Bacci S. Cellular and Molecular processes in wound healing. Biomedicines 2023;11:2526.

6. Rania Yassien DE, EI-Ghazouly D. The role of hesperidin on healing an incised wound in an experimentally induced diabetic adult male albino rats. Histological and immunohistochemical study. Egypt J Histol 2021;44:144-62.
7. Bonosi L, Silven MP, Biancardino AA, Sciortino A, Giammalva GR, Scerrati A, *et al*. Stem cell strategies in promoting neuronal regeneration after spinal cord injury: A systematic review. Int J Mol Sci 2022;23:12996.
8. Singh N, Divyanshu D, Saini S, Nagpal N, Tuli A, Bhatia N, *et al*. Pharmacological and therapeutic potential of hesperidin-a comprehensive review. Eur J Org Chem 2023;12:4499-537.
9. Jitendra G, Prabakaran L, Reena G, Mohan G. Nanoparticles formulation using counterion induced gelification technique: *In vitro* chloramphenicol release. Int Pharm Pharm Sci 2011;3:66-70.
10. Moradi SZ, Momtaz S, Bayrami Z, Farzaei MH, Abdollahi M. Nanoformulations of herbal extracts in treatment of neurodegenerative disorders. Front Bioeng Biotechnol 2020;8:238.
11. Bhati H, Bansal K, Bajpai M. Unveiling the various analytical techniques of polyphenols for pharmacological activity and nanotechnological delivery in wound healing. Curr Pharm Anal 2024;20:2021.
12. Ramadon D, McCrudden MT, Courtenay AJ, Donnelly RF. Enhancement strategies for transdermal drug delivery systems: Current trends and applications. Drug Deliv Transl Res 2022;12:758-91.
13. Garg R, Garg A. Tacrolimus loaded nanostructured lipid carriers using *Moringa oleifera* seed oil: Design, optimization and *in-vitro* evaluations. J Microencapsul 2023;40:502-16.
14. Guy RH. Drug delivery to and through the skin. Drug Deliv Transl Res 2024;14:2032-40.
15. Alkilani AZ, McCrudden MTC, Donnelly RF. Transdermal drug delivery: Innovative pharmaceutical developments based on disruption of the barrier properties of the stratum corneum. Pharmaceutics 2015;7:438-70.
16. Bahadur S, Sachan N, Harwansh RK, Deshmukh R. Nanoparticlized system: Promising approach for the management of Alzheimer's disease through intranasal delivery. Curr Pharm Des 2020;26:1331-44.
17. Jafari A, Daneshamouz S, Ghasemiyeh P, Mohammadi-Samani S. Ethosomes as dermal/transdermal drug delivery systems: Applications, preparation and characterization. J Liposome Res 2023;33:34-52.
18. Jain P, Taleuzzaman M, Kala C, Kumar Gupta D, Ali A, Aslam M. Quality by design (Qbd) assisted development of phytosomal gel of *Aloe vera* extract for topical delivery. J Liposome Res 2021;31:381-8.
19. Kaur J, Anwer MK, Sartaj A, Panda BP, Ali A, Zafar A, *et al*. ZnO nanoparticles of rubia cordifolia extract formulation developed and optimized with QbD application, considering *ex vivo* skin permeation, antimicrobial and antioxidant properties. Molecules 2022;27:1450.
20. Bansal K, Bhati H, Bajpai M. Pharmacological research - modern Chinese medicine new insights into therapeutic applications and nanoformulation approaches of hesperidin: An updated review. Pharmacol Res Mod Chin Med 2024;10:100363.
21. Sallam AN, Omari DM. Preformulation considerations in pharmaceutical formulation process. In: Nayak AK, Sen KK, editor. Dosage Forms, Formulation Developments and Regulations. Ch. 13. United States: Academic Press; 2024. p. 395-441.
22. White WP. Melting point determination. Am J Sci. 1909;28:453-73.
23. Chimagave SS, Jalalpure SS, Patil AK, Kurangi BK. Development and validation of stability indicating UV-spectrophotometric method for the estimation of hesperidin in bulk drugs, plant extract, ayurveda formulation and nanoformulation. Indian J Pharm Educ Res 2022;56:865-72.
24. Khan S, Khan S, Khan L, Farooq A, Akhtar K, Asiri AM. Fourier transform infrared spectroscopy: Fundamentals and application in functional groups and nanomaterials characterization. In: Handbook of Materials Characterization. Germany: Springer; 2018. p. 317-44.
25. Touitou E, Dayan N, Bergelson L, Godin B, Eliaz M. Ethosomes - novel vesicular carriers for enhanced delivery: Characterization and skin penetration properties. J Control Release 2000;65:403-18.
26. Andleeb M, Shoaib Khan HM, Daniyal M. Development, characterization and stability evaluation of topical gel loaded with ethosomes containing *Achillea millefolium* L. extract. Front Pharmacol 2021;12:603227.
27. Journal I, Sciences B, Chappidi SR, Education P. Formulation and *In vitro* evaluation of liposomes containing metformin hydrochloride. Int J Res Pharm Biomed Sci 2016;4:479-85.
28. Lim Y, Chew I, Choong T, Ching T, Tan KW. NanoCrystalline cellulose isolated from oil palm empty fruit bunch and its potential in cadmium metal removal. MATEC Web Conf 2016;59:4002.
29. Ascenso A, Raposo S, Batista C, Cardoso P, Mendes T, Praça FG, *et al*. Development, characterization, and skin delivery studies of related ultradeformable vesicles: Transfersomes, ethosomes, and transethosomes. Int J Nanomedicine 2015;10:5837-51.
30. Pathan IB, Jaware BP, Shelke S, Ambekar W. Curcumin loaded ethosomes for transdermal application: Formulation, optimization, *in-vitro* and *in-vivo* study. J Drug Deliv Sci Technol 2018;44:49-57.
31. El-Menshawe SF, Sayed OM, Abou-Taleb HA, El Tellawy N. Skin permeation enhancement of nicotinamide through using fluidization and deformability of positively charged ethosomal vesicles: A new approach for treatment of atopic eczema. J Drug Deliv Sci Technol 2019;52:687-701.
32. Garg BJ, Garg NK, Beg S, Singh B, Katare OP. Nanosized ethosomes-based hydrogel formulations

of methoxsalen for enhanced topical delivery against vitiligo: Formulation optimization, *in vitro* evaluation and preclinical assessment. J Drug Target 2016;24:233-46.
33. Andrade C. Understanding the difference between standard deviation and standard error of the mean, and knowing when to use which. Indian J Psychol Med 2020;42:409-10.
34. Gupta P, Kushwaha P, Hafeez A. Development and characterization of topical ethosomal gel for improved antifungal therapeutics. J Mol Liq 2024;405:125111.
35. Fathalla D, Youssef EM, Soliman GM. Liposomal and ethosomal gels for the topical delivery of anthralin: Preparation, comparative evaluation and clinical assessment in psoriatic patients. Pharmaceutics 2020;12:446.
36. Iizhar SA, Syed IA, Satar R, Ansari SA. *In vitro* assessment of pharmaceutical potential of ethosomes entrapped with terbinafine hydrochloride. J Adv Res 2016;7:453-61.
37. Vang Mouritzen M, Jenssen H. Optimized scratch assay for *in vitro* testing of cell migration with an automated optical camera. J Vis Exp 2018;138:57691.
38. Chaturvedi S, Garg A, Verma A. Nano lipid based carriers for lymphatic voyage of anti-cancer drugs: An insight into the *in-vitro*, *ex-vivo*, *in-situ* and *in-vivo* study models. J Drug Deliv Sci Technol 2020;59:101899.
39. Ataide JA, Geraldes DC, Gérios EF, Bissaco FM, Cefali LC, Oliveira-Nascimento L, *et al*. Freeze-dried chitosan nanoparticles to stabilize and deliver bromelain. J Drug Deliv Sci Technol. 2021;61:102225.
40. Rigon RB, Fachinetti N, Severino P, Santana MH, Chorilli M. Skin delivery and *in vitro* biological evaluation of trans-resveratrol-loaded solid lipid nanoparticles for skin disorder therapies. Molecules 2016;21:E116.
41. Ali SH, Sulaiman GM, Al-Halbosiy MM, Jabir MS, Hameed AH. Fabrication of hesperidin nanoparticles loaded by poly lactic co-Glycolic acid for improved therapeutic efficiency and cytotoxicity. Artif Cells Nanomed Biotechnol 2019;47:378-94.
42. Vazquez-Zapien GJ, Martinez-Cuazitl A, Granados-Jimenez A, Sanchez-Brito M, Guerrero-Ruiz M, Camacho-Ibarra A, *et al*. Skin wound healing improvement in diabetic mice through FTIR microspectroscopy after implanting pluripotent stem cells. APL Bioeng 2023;7:16109.
43. Danaei M, Dehghankhold M, Ataei S, Hasanzadeh Davarani F, Javanmard R, Dokhani A, *et al*. Impact of particle size and polydispersity index on the clinical applications of lipidic nanocarrier systems. Pharmaceutics 2018;10:57.
44. Paliwal S, Tilak A, Sharma J, Dave V, Sharma S, Yadav R, *et al*. Flurbiprofen loaded ethosomes - transdermal delivery of anti-inflammatory effect in rat model. Lipids Health Dis 2019;18:133.
45. Barupal AK, Gupta V, Ramteke S. Preparation and characterization of ethosomes for topical delivery of aceclofenac. Indian J Pharm Sci 2010;72:582-6.
46. Nasri S, Ebrahimi-Hoseinzadeh B, Rahaie M, Hatamian Zarmi A, Sahraeian R. Thymoquinone-loaded ethosome with breast cancer potential: Optimization, *in vitro* and biological assessment. J Nanostruct Chem 2020;10:19-31.

Source of Support: Nil. **Conflicts of Interest:** None declared.